$^{18}O_2$ labeling experiments illuminate the oxidation of *ent*-kaurene in bacterial gibberellin biosynthesis

Raimund Nagel and Reuben J. Peters*

Roy J. Carver Department of Biochemistry, Biophysics, and Molecular Biology, Iowa State University, Ames, IA, 50011, USA. *E-mail: rjpeters@iastate.edu

Abstract

Bacteria can produce gibberellin plant hormones. While the bacterial biosynthetic pathway is similar to that of plants, the individual enzymes are very distantly related and arose via convergent evolution. The cytochromes P450 (CYPs) that catalyze the multi-step oxidation of the alkane precursor *ent*-kaurene (**1**) to *ent*-kauren-19-oic acid (**5**), are called *ent*-kaurene oxidase (KO), and in plants are from the CYP701 family, and share less than 19% amino acid sequence identity with those from bacteria, which are from the phylogenetically distinct CYP117 family. Here the reaction series catalyzed by CYP117 was examined by $^{18}O_2$ labeling experiments, the results indicate successive hydroxylation of **1** to *ent*-kauren-19-ol (**2**) and then *ent*-kauren-19,19-diol (**3**) and most likely an intervening dehydration to *ent*-kauren-19-al (**4**) prior to the concluding hydroxylation to **5**. Accordingly, the bacterial and plant KOs converged on catalysis of the same series of reactions, despite their independent evolutionary origin.

Introduction

Gibberellins are essential plant hormones that regulate growth and development,[1, 2] but are also produced by plant-associated microbes, both fungi and bacteria.[3] Recently a cytochrome P450 (CYP) rich operon, responsible for gibberellin production, has been characterized from several bacteria.[4-7] Some of these are beneficial rhizobia, which engage in symbiosis with legumes to fix nitrogen in specialized root nodules,[8] while the others are plant pathogens that use gibberellin to suppress the plant defense

reaction during infection.[4, 9] The gibberellin biosynthetic pathway of plants, fungi and bacteria are highly similar in their intermediates, but seem to have independently evolved as the relevant enzymes are either from different enzymatic classes or belong to different families within the same class, but share very low overall sequence identity.[5]

The first oxidative steps in gibberellin biosynthesis is carried out by CYPs termed *ent*-kaurene oxidases (KOs), as these produce *ent*-kaur-16-en-19-oic acid (**5**) from *ent*-kaur-16-ene (**1**), via the intermediates *ent*-kaur-16-en-19-ol (**2**) and *ent*-kaur-16-en-19-al (**4**).[5] The bacterial KOs are from the CYP117 family, while the plant KOs are members of the CYP701 family and the fungal KOs from the CYP503 family.[2, 10, 11] Despite all falling within the CYP super-family, these CYP families share less than 20% sequence identity and are more similar to other CYP families from the same biological kingdom than to each other[5]. Indeed, while the plant and fungal KOs are typical eukaryotic CYPs, with N-terminal transmembrane helices, the CYP117 family members are typical soluble prokaryotic CYPs. Thus, the plant and bacterial KOs appear to have arisen via independent evolution, in parallel from the CYP super-family, despite their convergence on functionally analogous activity (i.e., **1** → **5**).

CYPs are heme proteins that act as monooxygenases. Upon substrate binding, CYPs undergo a one electron reduction, followed by binding of dioxygen. This triggers another one electron reduction and formation of one water molecule and the active ferryl-oxo state [Fe(IV)], also called compound I. The activated oxygen is then most often inserted into a C-H bond.[12, 13] There are however CYPs that either catalyze more complex and/or sequential reactions, such as the *ent*-kaurene oxidases.[14-17]

CYPs that catalyze the sequential oxidation of a methyl group to a carboxylic acid in theory can do so by any one of several pathways, with those for the formation of **5** from **1** depicted in Figure 1. The pathway taken by the KO from the plant *Arabidopsis thaliana*, CYP701A3, was previously characterized by $^{18}O_2$ labeling studies,[10] while the pathway for the fungal enzyme has not yet been investigated in this manner. The results indicated that, following initial hydroxylation of **1** to **2**, CYP701A3 then further hydroxylates **2** to the di-hydroxy *ent*-kaur-16-en-19-diol **(3)**, that undergoes dehydration to form **4**, which

is then directly hydroxylated to produce **5**. However, although the plant and bacterial *ent*-kaurene oxidases catalyze the same overall reaction (i.e., **1** → **5**), their independent/parallel evolutionary origins leaves open the possibility that they might use distinct mechanisms (i.e., series of reactions).

Here the series of reactions catalyzed by CYP117 was investigated via $^{18}O_2$ labeling experiments and the potential interaction of CYP117 with the upstream *ent*-kaurene synthase was analyzed by a metabolic engineering approach.

Results

Previous work with CYP117 family members from various bacterial species indicated that only those from plant pathogens are readily expressed in *E. coli*.[4-6] This may be due to the common phylogenetic origin of these phytopathogens with *E. coli*, which all fall within the gamma-proteobacteria class. Given that one of these, *Erwinina tracheiphila*, further falls within the same Enterobacteriaceae family as *E. coli*, and the CYP117 from this species exhibited better activity in previous recombinant whole-cell feeding studies with about 60% turnover, this *Et*CYP117 was chosen for mechanistic studies. For this purpose, a synthetic, codon-optimized gene was obtained for *Et*CYP117. To enable purification, a number of His-tag variants were constructed. Initial whole-cell feeding studies indicated that only the construct with a short C-terminal His-tag was functionally expressed. However, it was not possible to carry out in vitro assays. Even with this optimal construct, cell-free lysates exhibited inconsistent activity, did not bind to Ni-NTA resin, and instead of the characteristic absorbance maximum at 450 nm after reduction and CO binding, a broad absorbance between 400 and 410 nm either before or after addition of dithionite and/or CO was observed (**Supplemental Figure S1**). Accordingly, the studies described here were carried out using this *Et*CYP117 construct in whole-cell feeding assays conducted under an $^{18}O_2$ atmosphere.

To enable analysis by GC-MS, organic extracts of the cultures were methylated – i.e., to generate the methyl ester derivative of **5**. Upon feeding the intermediates **2** and **4** 40-50% turnover was observed. However, only ~5% turnover was observed with **1**. When **1** or **2** were used as substrates no

intermediates were found (i.e., **2** or **4**), and only **5** is observed as the product in all assays (**Figure 2**). This indicates that the intermediates are not released from the *Et*CYP117 active site during the course of the multiple reaction cycles necessary for the transformation of **1** to **5**.

The incorporation of ^{18}O into **5** was determined via analysis of the molecular ion of the methyl ester derivative [M^+; *m/z* 316], as well as two smaller fragments in which both oxygen atoms are retained, namely [M^+ -15; *m/z* 301] and [M^+ -43; *m/z* 273], which represent the loss of the methyl group at C-20 and loss of the D-ring, respectively.[18] The next lower mass fragment [M^+ -59; *m/z* 257] is generated from the loss of the methylated carboxylate, so both oxygen atoms, and therefore the labels, are lost. Incorporation of ^{18}O depended on the fed substrate and was consistent for all three fragments. Although in all experiments ~4-10% unlabeled **5** was observed, this presumably arises from the presence of ~3% unlabeled species in the oxygen source, along with the residual oxygen in the *E. coli* cultures that were used for these experiments. Thus, with **1** it appears that two ^{18}O were incorporated into **5**, while with **2** a mixture of one and two ^{18}O labels was observed (in a ~2.6:1 ratio), and with **4** only one ^{18}O label was observed (**Table 1** and **Figure 2**).

The low turnover of **1** suggested that CYP117, which is a soluble enzyme, may have trouble accessing this highly hydrophobic substrate, which should largely partition into the hydrophobic interior of membranes, particularly when **1** is exogenously fed. Although some diffusion and even volatilization of **1** has been reported,[19] in the context of the full pathway, it seemed possible that CYP117 might interact with the upstream *ent*-kaurene synthase (KS) to enhance its access to **1**. This was investigated via a metabolic engineering approach in which *Et*CYP117 was co-expressed with a KS in *E. coli,* also engineered to produce the KS substrate *ent*-copalyl diphosphate. When using the KS from the same origin (i.e., *E. tracheiphila*, *Et*KS), the relative amount of **1** converted to **5** by *Et*CYP117 was increased, albeit only to ~10% (**Figure 3A**). While greater turnover was observed, this modest increase was hypothesized to be simply due to endogenous production of **1** inside, versus exogenous addition outside, the *Et*CYP117 expressing cells. This was investigated by use of the KS from the plant *A. thaliana* (*At*KS), as this has very

low sequence identity, even over its single domain that corresponds to *Et*KS (*At*KS has two other domains that are relictual[20]), and is not expected to interact with *Et*CYP117. While *E. coli* co-expressing *At*KS instead of *Et*KS produced more than double the amount of **1** and **5**, the relative turnover from **1** to **5** was again ~10% (**Figure 3B**). Accordingly, *Et*CYP117 appears to simply access its hydrophobic substrate **1** via the presumably relatively small amounts that diffuse into the cytoplasm.

Discussion

While recombinantly expressed *Et*CYP117 did not appear to be stably folded in cell-free assays, it was possible to probe the series of reactions catalyzed by this multifunctional bacterial KO via whole-cell feeding studies carried out under an $^{18}O_2$ atmosphere. Given the evident initial insertion of oxygen into the olefinic substrate **1** to produce the alcohol **2**, it is the subsequently catalyzed reactions that are in question. Notably, the lack of detectable intermediates indicates that these are not released from the active site of CYP117 during the course of the overall transformation of **1** to **5**. Moreover, the production of doubly-labeled **5** from **1** demonstrates the use of at least two hydroxylation reactions, and rules out the use of two dehydrogenation reactions (i.e., **2** → **4** → **3** → **5**; **Supplemental Figure S2** and **Supplemental Table S2**).

The insertion of oxygen from $^{18}O_2$ in the transformation of **4** to **5** shows that this step represents a hydroxylation reaction. While this could proceed via hydroxylation of the equilibrating geminal-diol **3** to produce the *ortho*-acid hydrate **6** that then undergoes dehydration to **5**, the observed almost complete labeling by ^{18}O is in better agreement with the expected 100% incorporation resulting from direct hydroxylation of the aldehyde (**Supplemental Figure S2** and **Supplemental Table S4**). Consistent with the ability of CYPs to carry out such direct hydroxylation of an aldehyde to the corresponding acid, it has been previously demonstrated that a CYP catalyzes hydroxylation of 11-oxo-Δ^8-tetrahydrocannabinol to an acid without intervening generation of the geminal-diol.[21] Use of the alternative mechanism (i.e., **4** → **3** → **6** → **5**) would require almost completely selective retention of the most recently inserted oxygen.

While the observed ratio of 2.7:1 singly- and doubly- labeled **5** observed with **2** as the substrate does not directly conform to any of the potential reaction series (**Supplemental Figure S2** and **Supplemental Table S3**), the presence of doubly-labeled **5** demonstrates that this transformation can proceed via dual hydroxylation reactions. This requires loss of one of the two inserted oxygens via dehydration, either of **3** to **4** that would be expected to lead to a 1:1 ratio of singly- to doubly- labeled **5**, or of **6** to **5** that should result in a 2:1 ratio, which is closer to the observed ratio of 2.6:1. However, the lack of complete selectivity argues against **6** → **5**, as this would require essentially complete retention of the last oxygen to be inserted (as noted above), along with preferential, but not completely selective loss of one of the two other hydroxyl groups, which seems difficult to envision. In particular, if the most recently added hydroxyl in **6** is fixed in the active site to prevent its loss, it seems most likely that the hydroxyl to be removed also would be specified by this strict binding mode. It seems more plausible that, consistent with the observed ratio, the hydroxyl formed in conversion of **2** to **3** is preferentially removed, with such dehydration enabling correct orientation of the resulting **4** for subsequent hydroxylation to form **5**. Indeed, a plant KO has been shown to stereoselectively remove the *pro-R* hydrogen in conversion of **2** to **4**,[22] and stereoselective dehydration has been shown for CYP catalyzed conversion of testosterone to androstenedione,[23] as well as C-19 demethylation in estrogen biosynthesis.[24] Thus, while the alternative dehydration of **6** to **5** cannot be entirely ruled out, it seems most likely that *Et*CYP117 generally proceeds via stereoselective dehydration of **3** to **4**. Alternatively, it also is possible that *Et*CYP117 utilizes a mixed pathway, occasionally proceeding via oxidation of **2** to directly form **4**, which would then involve only a single insertion of oxygen and might help explain the prevalence of singly-labeled **5**. However, particularly given the requisite and demonstrated use of hydroxylation in the first and last transformations (i.e., **1** → **2** and **4** → **5**), along with the known propensity of CYPs to catalyze such insertion of oxygen,[12] it seems somewhat unlikely that this mechanistically distinct reaction is catalyzed to any significant extent by *Et*CYP117. Regardless, the observed incorporation of two oxygens in the

conversion of **2** to **5** demonstrates that the overall transformation of **1** to **5** can proceed via three hydroxylation reactions.

Overall, although alternative reaction series cannot be completely excluded, the results reported here suggest that the overall series of transformations catalyzed by *Et*CYP117 most likely is **1** → **2** → **3** → **4** → **5**. This implies that CYP117 catalyzes three hydroxylation reactions with an intervening dehydration of **3** to **4**. Accordingly, both the plant and bacterial KOs seem to catalyze the same series of reactions, although CYP117 appears to be stereoselective in the dehydration step, which contrasts with the plant KO.[10] Regardless, while this congruence further highlights the similarities between the independently evolved biosynthesis of gibberellins in bacteria and plants, it also is perhaps not so surprising, as it may simply reflect the preferential insertion of oxygen (i.e., hydroxylation) catalyzed by CYPs.[12]

Experimental

Cloning of CYP117

The codon optimized version of *Et*CYP117 was a gift from Manus Biosynthesis and was PCR amplified using Q5 HotStart High-Fidelity DNA polymerase (NEB) and cloned into the Invitrogen pET expression system vectors pET100 and pET101 (Thermo-Fisher Scientific), for expression with either N- or C-terminal His-Tags encoded by each vector, respectively. Alternatively, a 6xHis-Tag was inserted before the stop codon by PCR, and this construct cloned into pET101. The primer sequences are given in **Supplementary Table 1**. This latter PCR product was cloned into pENTR/SD/D-TOPO (Thermo-Fisher Scientific). The gene was then PCR amplified with Q5 HotStart High-Fidelity DNA polymerase (NEB) and M13 primers, gel purified and used for a Gateway reaction with the Gateway LR Clonase II Enzyme Mix (Thermo-Fisher Scientific) and pCOLADuet-1/DEST, which was generated by restriction digestion of pCOLADuet-1 (Novagen) with NcoI and NotI, the restriction sites blunt-ended with T4 DNA Polymerase (NEB), and ligate with the Reading Frame A Cassette of the Gateway Vector Conversion System (Thermo-Fisher Scientific).

Expression of CYP117

CYP117 in pET100 or pET101 was transformed into *E. coli* BL21-(Star) cells for expression, 3 colonies were selected for inoculation of a 10 mL starter-culture in NZY medium (10 g/L NaCl, 10 g /L casein, 5 g/L yeast extract, 1 g/L $MgSO_4$ (anhydrous), pH 7.0) with 50 µg/mL carbenicillin, which was incubated for 2 days at 18°C and 200 rpm. 5 ml of the starter culture was transferred to 100 ml fresh NZY with 50 µg/mL carbenicillin, the culture was induced at OD 0.8-0.9 with 1 mM IPTG, and assist CYP expression 1 mM aminolevulinic acid, 1 mM riboflavin and 0.1 mM $FeCl_3$ were added. After induction, cultures were incubated at 18°C and 200 rpm for 12 hours.

For protein purification attempts, recombinant cells were harvested by centrifugation for 30 min at 5000 x *g* and taken up in 10 mL 50 mM phosphate buffer pH 7.5, then lysed either by freeze thawing with the addition of 10 mg lysozyme (Sigma-Aldrich), sonication, or by homogenization with an EmulsiFlex C-5 (Avestin, Canada). The resulting lysate was passed over a 1 mL Ni-NTA agarose (Qiagen), the column was washed with 50 mM phosphate buffer pH 7.5 including either 10 or 50 mM imidazole. Protein was eluted with 250 mM imidazole in 50 mM phosphate buffer pH 7.5.

For metabolic engineering, *E. coli* C41 OverExpress (Lucigen) cells were transformed with pGG*e*C, pIRS, pCOLA-Duet1/DEST::*Et*CYP117, and either pET100::*Et*KS or pDEST14::*At*KS. Cultures of the resulting recombinant strains were grown and products extracted and analyzed as described previously.[6, 25]

$^{18}O_2$ labeling experiments

50 ml cultures were induced at OD 0.8 with 1 mM IPTG for 2 hrs before being centrifuged at 4000 x g for 10 min at 4°C and taken up in 10 mL NZY medium that had been freshly degassed under vacuum. Amber 10 mL glass vials were purged with nitrogen, and then 2 ml degassed NZY and 100 µL ethanol containing 1 mg/mL of **2** or **4** added. For **1** as substrate, assays used larger vials (50 mL), with 20 mL degassed NZY and 200 µL of ethanol with 1 mg/mL of **1** added. In each case, the vial was again purged with nitrogen and then sealed with a crimped rubber septum. $^{18}O_2$ (97% labeled, Sigma-Aldrich, pressurized to less than 2.4 bar) was introduced into the vial from the compressed gas cylinder via a syringe needle until

pressure between the tank and the vial equalized. Then the resuspended cells were added to the vial using a syringe. In the case of assays with **2** or **4**, 200 µL were added, while for assays with **1** this was increased to 5 mL. $^{18}O_2$ was added two additional times, as described above, in time intervals of 8 h, before the reaction was stopped by addition of an equal volume of 5N HCl as the cell resuspension (i.e., 200 µL for assays with **2** or **4**, or 5 mL for assays with **1**). The assay was extracted three times with 2 or 25 mL of hexanes (for assays with **2** or **4** versus **1**, respectively), which were combined and evaporated to dryness. The residues were taken up in 200 µL tert-butyl-methyl ether (Sigma-Aldrich) and methylated to **5** with addition of 50 µL of a trimethylsulfonium hydroxide solution (Sigma-Aldrich). Products were analyzed by GC-MS as described previously.[4]

Conflict of Interest

There are no conflicts to declare

Acknowledgements

The authors thank Manus Biosynthesis for the codon optimized version of CYP117 and Meimei Xu for construction of pCOLADuet1/DEST. This work was supported by a grant from the NSF (CHE-1609917) to R.J.P., along with a postdoctoral fellowship to R.N. from the Deutsche Forschungsgemeinschaft (DFG) NA 1261/1-2.

Literature/References

1. P. Hedden and V. Sponsel, *J Plant Growth Regul*, 2015, **34**, 740-760.
2. P. Hedden and S. G. Thomas, *Biochem. J.*, 2012, **444**, 11-25.
3. P. Hedden, A. L. Phillips, M. C. Rojas, E. Carrera and B. Tudzynski, *J Plant Growth Regul*, 2001, **20**, 319-331.
4. R. Nagel, P. C. Turrini, R. S. Nett, J. E. Leach, V. Verdier, M. A. Van Sluys and R. J. Peters, *New Phytol*, 2017, **214**, 1260-1266.
5. R. S. Nett, M. Montanares, A. Marcassa, X. Lu, R. Nagel, T. C. Charles, P. Hedden, M. C. Rojas and R. J. Peters, *Nat Chem Biol*, 2017, **13**, 69-74.
6. R. Nagel and R. J. Peters, *Mol Plant Microbe Interact*, 2017, **30**, 343-349.
7. Y. Tatsukami and M. Ueda, *Sci Rep*, 2016, **6**, 27998.
8. R. S. Nett, T. Contreras and R. J. Peters, *ACS Chem.Biol.*, 2017, **12**, 912-917

9. X. Lu, D. M. Hershey, L. Wang, A. J. Bogdanove and R. J. Peters, *New Phytol.*, 2015, **206**, 295-302.
10. D. Morrone, X. Chen, R. M. Coates and R. J. Peters, *Biochem. J.*, 2010, **431**, 337-344.
11. B. Tudzynski, P. Hedden, E. Carrera and P. Gaskin, *Appl Environ Microbiol*, 2001, **67**, 3514-3522.
12. P. R. Ortiz de Montellano, *Cytochrome P450 - Structure, Mechanism, and Biochemistry*, Springer International Publishing, 4 edn., 2015.
13. I. G. Denisov, T. M. Makris, S. G. Sligar and I. Schlichting, *Chem. Rev.*, 2005, **105**, 2253-2277.
14. M. Mizutani and F. Sato, *Arch. Biochem. Biophys.*, 2011, **507**, 194-203.
15. D. K. Ro, G. I. Arimura, S. Y. W. Lau, E. Piers and J. Bohlmann, *Proc. Natl. Acad. Sci. U. S. A.*, 2005, **102**, 8060-8065.
16. D. K. Ro, E. M. Paradise, M. Quellet, K. J. Fisher, K. L. Newman, J. M. Ndungu, K. A. Ho, R. A. Eachus, T. S. Ham, J. Kirby, M. C. Y. Chang, S. T. Withers, Y. Shiba, R. Sarpong and J. D. Keasling, *Nature*, 2006, **440**, 940-943.
17. R. A. Stearns, P. K. Chakravarty, R. Chen and S. H. L. Chiu, *Drug Metab. Dispos.*, 1995, **23**, 207-215.
18. P. Gaskin and J. MacMillan, *GC-MS of the gibberellins and related compounds : methodology and a library of spectra*, Univ. of Bristol (Cantocks Enterprises Ltd), Bristol, 1991.
19. M. Otsuka, H. Kenmoku, M. Ogawa, K. Okada, W. Mitsuhashi, T. Sassa, Y. Kamiya, T. Toyomasu and S. Yamaguchi, *Plant Cell Physiol.*, 2004, **45**, 1129-1138.
20. D. M. Hershey, X. Lu, J. Zi and R. J. Peters, *J Bacteriol*, 2014, **196**, 100-106.
21. K. Watanabe, S. Narimatsu, I. Yamamoto and H. Yoshimura, *J. Biol. Chem.*, 1991, **266**, 2709-2711.
22. P. F. Sherwin and R. M. Coates, *J. Chem. Soc., Chem. Commun.*, 1982, 1013-1014.
23. A. W. Wood, D. C. Swinney, P. E. Thomas, D. E. Ryan, P. F. Hall, W. Levin and W. A. Garland, *J. Biol. Chem.*, 1988, **263**, 17322-17332.
24. M. Akhtar, M. R. Calder, D. L. Corina and J. N. Wright, *Biochem. J.*, 1982, **201**, 569-580.
25. D. Morrone, L. Lowry, M. K. Determan, D. M. Hershey, M. Xu and R. J. Peters, *Appl. Microbiol. Biotechnol.*, 2010, **85**, 1893-1906.

Table 1

Percent ^{18}O isotopomers - methyl ester of *ent*-kaurenoic acid (5)

		substrate		
	m/z	*ent*-kaurene (**1**)	*ent*-kaurenol (**2**)	*ent*-kaurenal (**4**)
$[M^+ - C_3H_7]$	273	6 ± 2	7 ± 2	12 ± 3
	+2	6 ± 2	68 ± 4	86 ± 4
	+4	88 ± 3	25 ± 3	2 ± 1
$[M^+ - CH_3]$	301	5 ± 2	5 ± 2	11 ± 2
	+2	7 ± 2	70 ± 4	87 ± 4
	+4	88 ± 3	26 ± 3	2 ± 1
$[M^+]$	316	4 ± 2	8 ± 2	10 ± 2
	+2	5 ± 2	66 ± 4	88 ± 4
	+4	91 ± 3	26 ± 3	2 ± 1

Figures

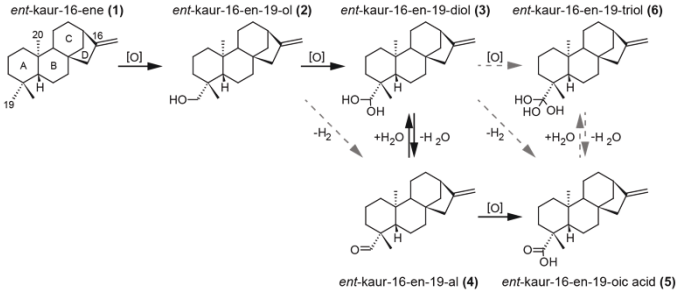

Figure 1: Potential reactions catalyzed by CYP117. Scheme showing all potential reactions for the transformation of *ent*-kaur-16-ene (**1**) to *ent*-kaur-16-en-19-oic acid (**5**), full arrows indicate the proposed pathway for the plant KO, CYP701A3 from *Arabidopsis thaliana*[9], the other possible pathways are indicated by dashed arrows.

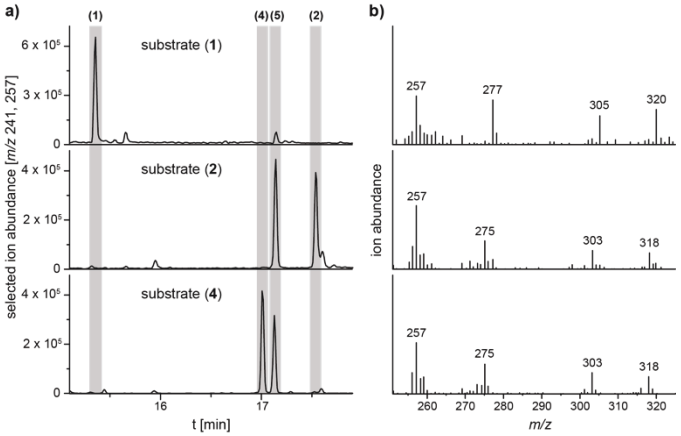

Figure 2: GC-MS analysis of $^{18}O_2$ labeling experiments with CYP117. (a) GC-chromatograms of CYP117 assays with *ent*-kaur-16-ene **(1)**, *ent*-kaur-16-en-19-ol **(2)** or *ent*-kaur-16-en-19-al **(4)** as substrate; **(b)** MS spectra of the methyl ester of the product *ent*-kaur-16-en-19-oic acid **(5)** showing the three fragments that retain ^{18}O labels and one fragment where the methylated carboxylate is lost.

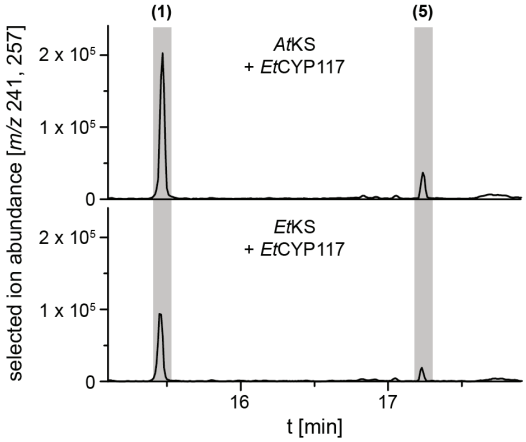

Figure 3: Substrate accessibility in metabolic engineering approach. (a) GC-chromatograms of organic extracts from *E. coli* cultures harboring plasmids for the production of **1** using either the relevant bacterial *ent*-kaurene synthase, *Et*KS, or unrelated plant analog, *At*KS, co-expressed with *Et*CYP117.

Graphical Abstract

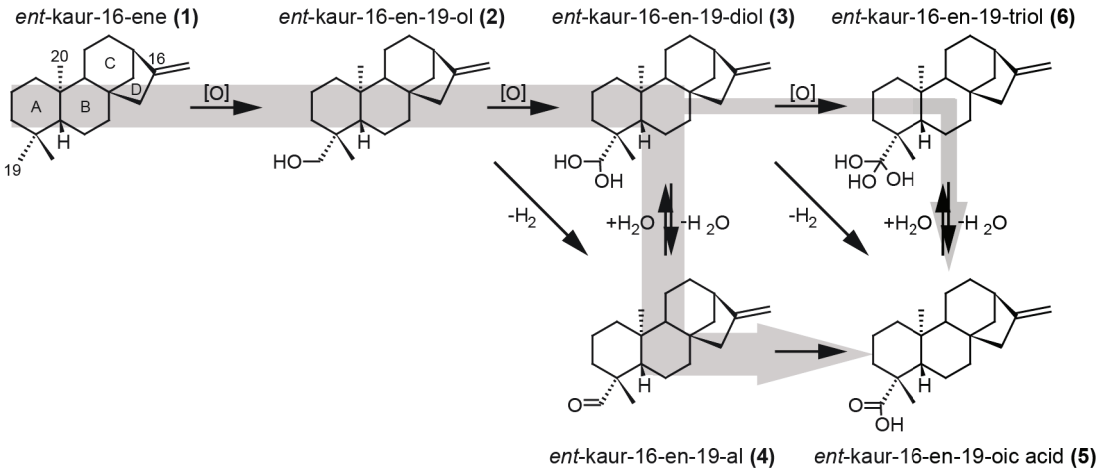

Supplemental Material for:

$^{18}O_2$ labeling experiments illuminate the oxidation of *ent*-kaurene in bacterial gibberellin biosynthesis

Nagel, Raimund and Peters, Reuben J.*

Roy J. Carver Department of Biochemistry, Biophysics, and Molecular Biology, Iowa State University, Ames, IA, 50011, USA. *E-mail: rjpeters@iastate.edu

Contents

S1 **Supplemental Table S1.** Primers for cloning of synthetic *Et*CYP117 into pET100/pET101.

S2 **Supplemental Table S2.** Theoretical labeling patterns from *ent*-kaurene.

S3 **Supplemental Table S3.** Theoretical labeling patterns from *ent*-kaurenol.

S4 **Supplemental Table S4.** Theoretical labeling patterns from *ent*-kaurenal.

S5 **Supplemental Figure S1.** Expression and spectroscopic properties of *Et*CYP117.

S5 **Supplemental Figure S2.** Theoretical position of ^{18}O.

Supplemental Table S1: Primers for cloning of synthetic *Et*CYP117 into pET100/pET101.

Primer name	Primer Sequence
forward	CACCATGGCGTTGCTGAACCCCTTTAAACG
reverse	TCATATGGACAGTGATCTACCTGCATCTTTTGAAAAAGC
reverse -stop	TATGGACAGTGATCTACCTGCATCTTTTGAAAAAGC
reverse +6xHistidine	TCAATGATGATGATGATGATGTATGGACAGTGATCTACCTGCATCTTTTGAAAAAGC

Underlined sequence in forward primer incorporated for dTOPO-based cloning method.

Supplemental Table S2: Potential labeling patterns from *ent*-kaurene, 1 (% isotopomer).

$[M^+]$	**(1) →**	**(2) →**	**(3) →**	**(6) →**	**(5)**
+0	100	0	0	0	0
+2	0	100	0	0	0
+4	0	0	100	0	100
+6	0	0	0	100	0
	(1) →	**(2) →**	**(3) →**	**(4) →**	**(5)**
+0	100	0	0	0	0
+2	0	100	0	100	0
+4	0	0	100	0	100
+6	0	0	0	0	0
	(1) →	**(2) →**	**(4) →**	**(3) →**	**(5)**
+0	100	0	0	0	0
+2	0	100	100	100	100
+4	0	0	0	0	0
+6	0	0	0	0	0
	(1) →	**(2) →**	**(4) →**	**(5)**	
+0	100	0	0	0	
+2	0	100	100	0	
+4	0	0	0	100	
+6	0	0	0	0	
	(1) →	**(2) →**	**(3) →**	**(5)**	
+0	100	0	0	0	
+2	0	100	0	0	
+4	0	0	100	100	
+6	0	0	0	0	

Supplemental Table S3: Potential labeling patterns from *ent*-kaurenol, 2 (% isotopomer).

$[M^+]$	**(2) →**	**(3) →**	**(6) →**	**(5)**
+0	100	0	0	0
+2	0	100	0	66
+4	0	0	100	33
	(2) →	**(3) →**	**(4) →**	**(5)**
+0	100	0	50	0
+2	0	100	50	50
+4	0	0	0	50
	(2) →	**(4) →**	**(5)**	
+0	100	100	0	
+2	0	0	100	
+4	0	0	0	
	(2) →	**(3) →**	**(5)**	
+0	100	0	0	
+2	0	100	100	
+4	0	0	0	

Supplemental Table S4: Potential labeling patterns from *ent*-kaurenal, 4 (% isotopomer).

$[M^+]$	**(4) →**	**(5)**		
+0	100	0		
+2	0	100		
+4	0	0		
	(4) →	**(3) →**	**(5)**	
+0	100	100	100	
+2	0	0	0	
+4	0	0	0	
	(4) →	**(3) →**	**(6) →**	**(5)**
+0	100	100	0	33
+2	0	0	100	66
+4	0	0	0	0

Supplemental Figure S1

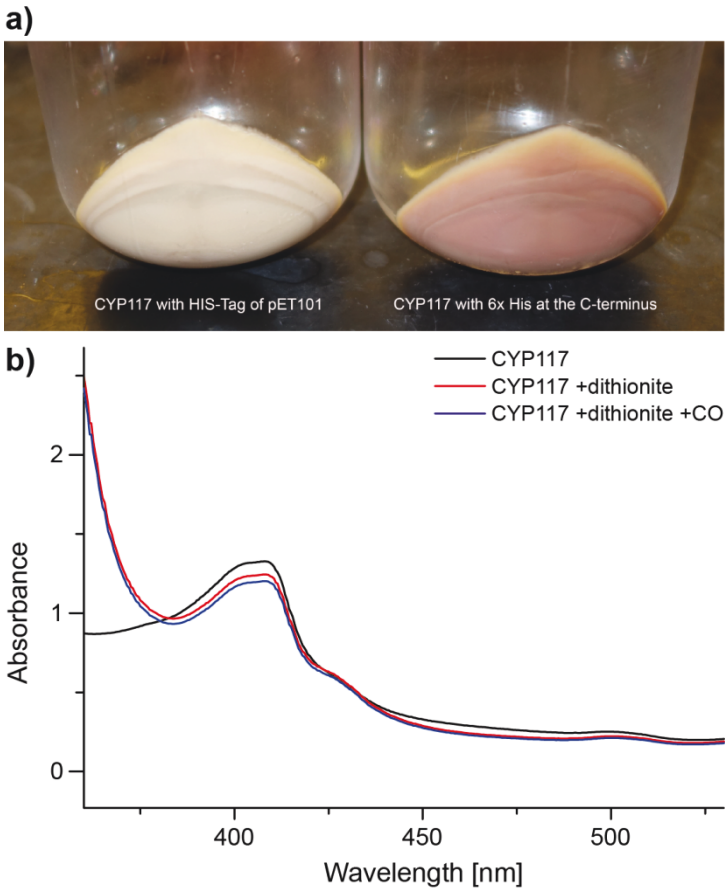

Supplemental Figure S1: Expression and spectroscopic properties of *Et*CYP117. (a) Cell pellets from *E. coli* cultures expressing *Et*CYP117 with the C-terminal His-Tag encoded by pET101, or only 6 histidines directly incorporated at the C-terminus (i.e., without any linker sequence). **(b)** UV-VIS absorbance measurement of E. coli cell lysate expressing *Et*CYP117 with the short 6xHis-tag, before and after reduction by dithionite, as well as subsequent addition of carbon monoxide (CO).

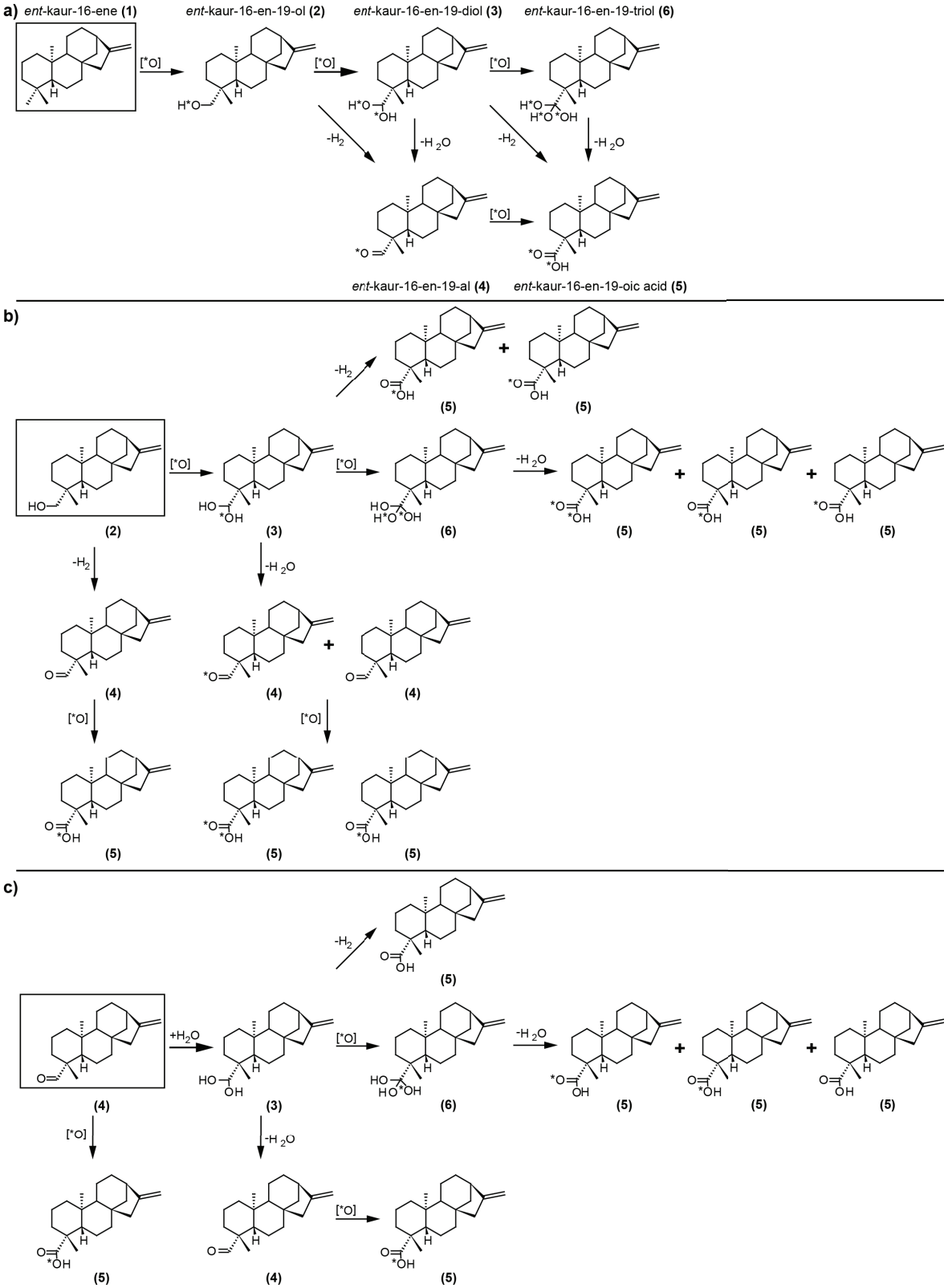

Supplemental Figure S2. Theoretical position of ^{18}O labels. Schemes depicting the position of the ^{18}O label, marked by an asterisk (*), for all pathways from *ent*-kaurene **(a)**, *ent*-kaurenol **(b)** or *ent*-kaurenal **(c)**. For **(a)** and **(b)** reverse reactions were omitted.